AUDIT, RESEARCH AND GUIDELINE UPDATE

CT features of pulmonary arterial hypertension and its major subtypes: a systematic CT evaluation of 292 patients from the ASPIRE Registry

S Rajaram,[1] A J Swift,[1] R Condliffe,[2] C Johns,[1] C A Elliot,[2] C Hill,[3] C Davies,[3] J Hurdman,[2] I Sabroe,[2] J M Wild,[1] D G Kiely[2]

ABSTRACT
We evaluated the prevalence and prognostic value of CT-pulmonary angiographic (CTPA) measures in 292 treatment naive patients with pulmonary arterial hypertension (PAH). Pulmonary artery calcification (13%) and thrombus (10%) were exclusively seen in PAH-congenital heart disease. Oesophageal dilation (46%) was most frequent in PAH-systemic sclerosis. Ground glass opacification (GGO) (41%), pericardial effusion (38%), lymphadenopathy (19%) and pleural effusion (11%) were common. On multivariate analysis, inferior vena caval area, the presence of pleural effusion and septal lines predicted outcome. In PAH, CTPA provides diagnostic and prognostic information. In addition, the presence of GGO on a CT performed for unexplained breathlessness should alert the physician to the possibility of PAH.

INTRODUCTION
Pulmonary hypertension (PH) ranges from a mild elevation in pressure in severe cardiac/respiratory disease to rare conditions where severe pressure elevation results in right heart failure and death. The current classification identifies 5 major groups, defining prognosis and treatment. Classification within groups is also important. In pulmonary arterial hypertension (PAH), survival in idiopathic PAH (IPAH) is superior to PAH associated with connective tissue disease (PAH-CTD) but inferior to PAH associated with congenital heart disease (PAH-CHD).[1]

Due to the heterogeneity of PH, imaging is recognised as a valuable tool improving phenotyping and providing prognostic information, complementing data from right heart catheterisation. Cardiac MR provides functional information whereas CT provides structural information, depicting features which may cause and be due to PH. Previous CT studies in PH have mainly been in mixed groups; only a small number of CT parameters have been studied and prognostic data are limited. Our objective was to systematically evaluate the prevalence, diagnostic and prognostic value of vascular, cardiac, parenchymal and mediastinal CT findings in patients with PAH at the time of diagnosis.

METHODS
Consecutive treatment naive patients with PAH were identified from the ASPIRE Registry[1] of patients referred to a PH referral centre. Classification was by standard criteria following multidisciplinary assessment. Inclusion criteria required the patient to have undergone multislice CT-pulmonary angiography (CTPA) and high resolution computed tomography (HRCT) within 3 months of initial diagnostic right heart catheterisation (RHC), except for Eisenmenger's syndrome in whom RHC was not routinely performed.

Image analysis and interpretation: see online supplement.

Vascular changes: Pulmonary artery to aorta ratio (PA to Ao ratio), depth of pericardial effusion, reflux of contrast into the hepatic veins and inferior vena cava (IVC) cross-sectional area were measured (figures 1 and 2).

Cardiac changes: Right ventricle to left ventricle ratio (RV to LV ratio), right atrial size, interventricular (IV) septal position and RV free wall thickness were recorded (figure 3).

Parenchymal and mediastinal changes: The presence of ground glass opacification (GGO) and the pattern/distribution was noted (figure 4). CT scans were assessed for fibrosis, pleural effusions, mediastinal lymphadenopathy and dilated bronchial collaterals.

RESULTS
Of 444 consecutive patients with PAH from the ASPIRE Registry (2006–2010), 292 patients had multislice CTPA/HRCT within 3 months of right heart catheterisation; mean age, 62 ± 16 years (table 1) (see online supplement for haemodynamic and demographic characteristics, figure 5 and online supplementary table S2).

Vascular changes
The PA to Ao ratio was highest for patients with PAH-CHD-Eisenmenger followed by IPAH. Greater IVC dilatation was observed in PAH-portal and PAH-CHD. Regurgitation of contrast into hepatic veins was frequent across the subgroups. PA calcification and mural thrombus were noted only in patients with PAH-CHD and occurred in 16% (calcification) and 13% (mural thrombus) in PAH-CHD-Eisenmenger group.

Cardiac changes
The RV to LV ratio for PAH was 1.25 ± 0.42 (mean $\pm$ SD) highest in IPAH although there were no statistically significant differences between groups. The RV wall thickness was 6 ± 2.7 mm for PAH and
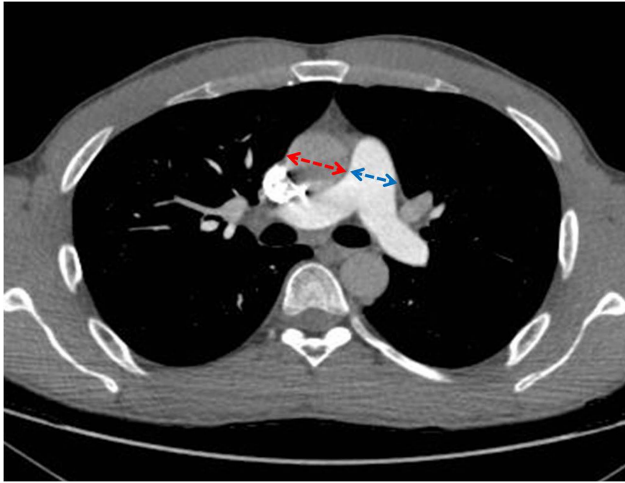
Figure 1 The pulmonary artery (PA) aorta ratio was obtained by measuring the widest transverse diameter of the PA (blue) and the corresponding transverse diameter of aorta (red).

within subgroups less RV hypertrophy was seen in PAH-CTD (PAH systemic sclerosis (PAH-SSc) and PAH-CTD-non-SSc). Mean right atrium (RA) size for PAH was 55 mm±12.1.

Qualitative grading of the RA showed 82% had right atrial enlargement. A higher proportion of patients with IPAH and PAH-CHD were graded as severe RA enlargement compared with other subgroups. Deviation of the IV septum towards the LV was evident in 27% of patients with PAH and most frequent in IPAH. A pericardial effusion was seen in 38% of patients most frequently in patients with PAH-CTD-non-SSc and least frequently in PAH-CHD-Eisenmenger.

Parenchymal and mediastinal changes

Ground glass opacities were frequent in PAH (41%), most commonly PAH-CHD. The predominant pattern of GGO in PAH was a centrilobular pattern. In PAH-SSc, 51% of patients had central distribution of GGO and 49% had non-central distribution; compared with a low occurrence of central distribution in other subgroups.

Dilated collateral vessels occurred most commonly in patients with PAH-CHD-Eisenmenger syndrome.

Survival results

The maximal duration of follow-up was 6 years (mean 3 years) and there were 112 deaths. Multivariable Cox proportional hazard analysis incorporating clinical, haemodynamic and CT parameters showed CT parameters, inferior vena caval area and
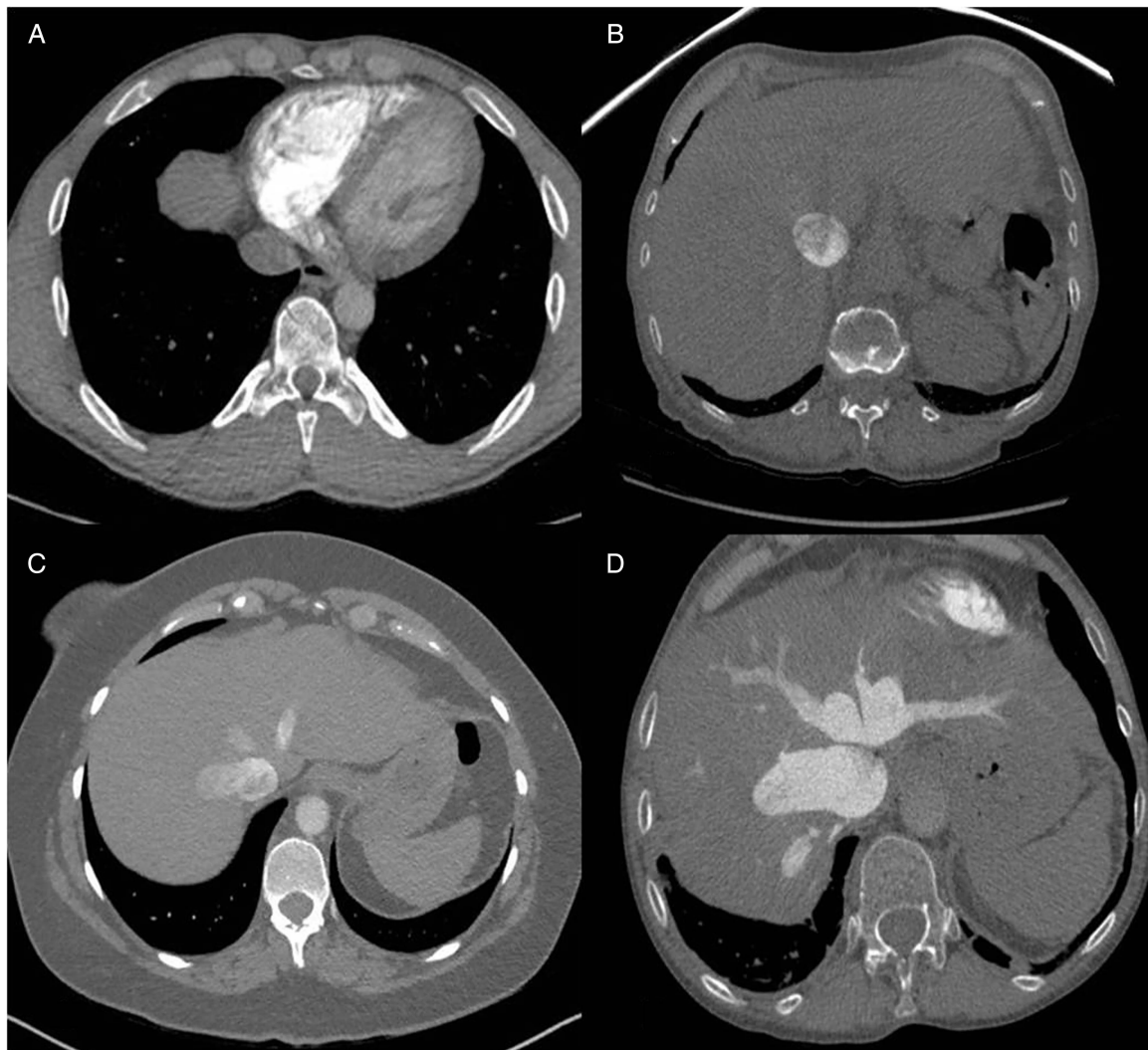
Figure 2 Grading of tricuspid regurgitation. (A) 0=There is no reflux into IVC, (B) 2=reflux into IVC but not hepatic veins, (C) 3=reflux into IVC and proximal hepatic veins and (D) 4=reflux into IVC and distal hepatic veins.
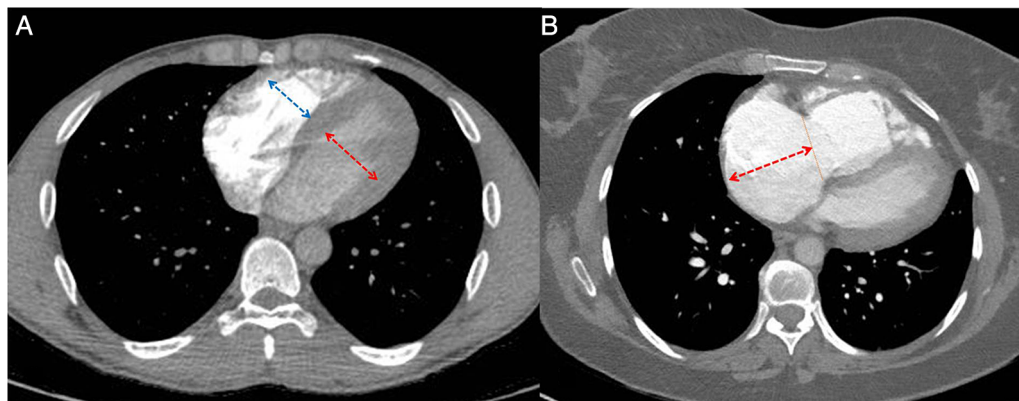
Figure 3 (A) The maximum mid-transverse diameters of the RV (right arrow) and LV (left arrow) cavities were measured in the axial plane at their widest points between the inner surfaces of the free wall and the interventricular septum. (B) For assessing the right atrial margin (arrow) on CT, right atrial length was measured from the centre of tricuspid annulus to the superior right atrial margin. RV, right ventricle; LV, left ventricle.

the presence of pleural effusion/septal lines to be significant predictors of death (see online supplementary tables S3 and S4 and figures 2 and 6).

DISCUSSION
This study is the first comprehensive report of the prevalence and relative prognostic value of vascular, cardiac, lung parenchymal and mediastinal changes on CT in PAH and its major subgroups. Within subgroups, different vascular and cardiac configurations are observed, reflecting the heterogeneity of PAH. We have demonstrated that cardiac and vascular morphology can predict outcome in PAH and CT measures such as IVC area, and pleural effusion/septal lines are independent prognostic markers.

In addition to established measures, quantifiable CT findings including elevated RV to LV ratio, deviated IV septum, dilated RA, RV free wall hypertrophy, pericardial/pleural effusions, contrast regurgitation into the hepatic veins and GGO occur frequently in PAH and major subgroups.

Different CT patterns were observed in PAH subgroups but none were diagnostic. IPAH and PAH-CHD-Eisenmenger have a higher proportion of severe RA dilatation, contrast regurgitation into hepatic veins and ground glass opacities. While more patients with IPAH have a deviated IV septum and greater RV to LV ratio, the Eisenmenger group had a higher PA to Ao ratio,

PA calcification, mural thrombus and dilated collateral vessels. Although the higher RV to LV ratio in IPAH may appear counterintuitive, this may reflect better preserved RV function in the conditioned RV of the Eisenmenger patient and the off-loading effect of a right-left shunt. We noted that central distribution of ground glass opacity was frequent in patients with PAH-SSc whereas a centrilobular pattern was more common in IPAH and PAH-CHD-Eisenmenger.

CT features predict outcome in treatment naive PAH including RV to LV ratio, right atrial size, IV septal position, inferior vena caval size, pericardial/pleural effusions, mediastinal lymphadenopathy and septal lines. Most of these parameters predict survival in major subgroups (see online supplementary table S4). IVC area the presence of pleural effusions/septal lines were predictors of outcome independent of pulmonary haemodynamics and WHO functional class, highlighting the prognostic value of CT.[2] In PAH, RV function is a prognostic determinant. IV septal displacement and dilatation of RV as shown by a high RV to LV ratio on CT reflect a failing RV and it is not surprising they have prognostic significance. A failing RV and tricuspid regurgitation elevate right atrial pressure. Inferior vena caval size was demonstrated to be a strong predictor of outcome. Vena caval diameter reflects the pressure in the RA[2] which is an important prognostic marker in PAH. Elevated right atrial pressure impedes mediastinal lymphatic and venous drainage resulting in the development of septal lines, mediastinal lymphadenopathy and pleural and pericardial
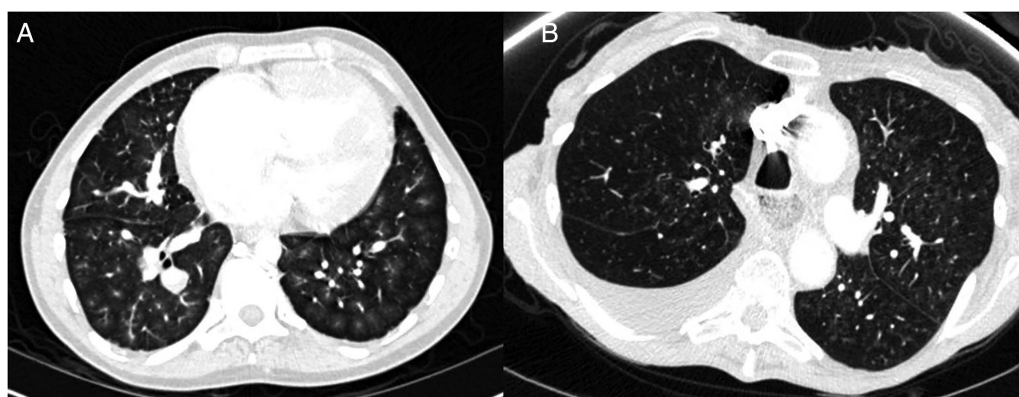
Figure 4 Centrilobular ground glass pattern (A) and central ground glass pattern (B).

Table 1 Features seen on CT-pulmonary angiography in patients with pulmonary arterial hypertension (PAH) and its major subgroups

CT parameters Vascular changes	PAH (n=292)	IPAH (n=74)	PAH-SSc (n=95)	PAH-CTD-non-SSc (n=39)	PAH-portal (n=14)	PAH-CHD (n=63)	PAH-CHD-Eisenmenger (n=31)
PA to Ao ratio~	1.16 (0.21)	1.19 (0.18)*	1.04 (0.16)*	1.07 (1.16)*	1.08 (0.17)*	1.26 (0.40)†‡*§*¶	1.46 (0.45)
IVC size (mm^2)~	596 (207)	583 (200)	570 (203)	546 (206)	632 (156)	647 (209)	659 (212)
TR present	73	80	67	62	57	85	93
Grade 1	18	15	20	23	36	14	16
Grade 2	21	24	23	15	14	19	23
Grade 3	12	16	13	13	0	8	22
Grade 4	22	24	12	10	7	44	32
Calcification in PA	3	0	0	0	0	13	16
Thrombus in PA	2	0	0	0	0	10	13
Cardiac changes							
RV to LV ratio	1.25 (0.42)	1.39 (0.46)	1.19 (0.48)	1.19 (0.36)	1.25 (0.35)	1.15 (0.30)	1.23 (0.38)
RVH (mm)	6 (2.7)	6 (2.3)‡	4 (1.78)*¶	4 (3.21)*	6 (1.89)	7 (4.26)§‡	8 (2.5)
RA size (mm)	55 (12.1)	57 (10.9)	53 (12.5)*	52 (13.1)*	56 (17.2)	59 (13.4)§‡	59 (14.6)
RA size							
Moderate	28	35	20	26	36	35	42
Severe	20	24	16	10	14	27	22
IV septum							
Flattened	31	42	24	26	43	30	29
Deviated	27	34	19	21	21	33	29
Pericardial effusion							
Present	38	38	36	53	42	48	30
Depth (mm)~	12 (5)	8 (7)	14 (6)	13 (6)	14 (5)	13 (4)	11 (4)
Lung and mediastinal changes							
GGO present	41	42	36	24	21	60	58
Central pattern**	21	10	51	10	2	5	6
Centrilobular pattern**	55	48	61	60	67	53	56
Collaterals vessel	11	9	1	8	0	35	55
Lymphadenopathy	19	22	25	27	0	10	16
Pleural effusion	11	14	15	8	14	5	3
Septal lines	21	30	23	5	21	18	23
Ascites	5	5	4	8	14	2	0
Oesophageal dilatation	23	7	46	36	7	6	10

Frequency is expressed as a percentage; for absolute values, data are expressed as mean (SD).
*p<0.05 in comparison with PAH-CHD.
†p<0.05 in comparison with PAH-portal.
‡p<0.05 in comparison with PAH-SSc.
§p<0.05 in comparison with PAH-CTD-non-SSc.
¶p<0.05 in comparison with IPAH.
**Represents percentage of the patients with GGO present.
Ao, aorta; CHD, congential heart disease; CTD, connective tissue disease; GGO, ground glass opacification; IPAH, idiopathic pulmonary arterial hypertension; IV, interventricular; IVC, inferior vena cava; LV, left ventricle; PA, pulmonary artery; PAH, pulmonary arterial hypertension; RA, right atrium; RV, right ventricle; RVH, right ventricular hypertrophy; TR, tricuspid regurgitation; SSc-systemic sclerosis.

Patients with PAH identified from ASPIRE
registry between Jan 2006 to Jan 2010 (n= 444)

HRCT only (n=60)
Single-slice CT (n= 12)
CT & RHC not within 3 months (n=33)
Non available CT (n= 47)

Study population (n=292)

Subcategories of PAH

❖Idiopathic PAH (n=74)
❖PAH-SSc (n=95)
❖Connective tissue disease not SSc (n=39)
  ●6 MCTD
●7 RA
●7 SLE
●6 UCTD
●8 overlap
●5 other

❖PAH congenital (n=63) *
  ●31 Eisenmenger (9ASD,15VSD,9others-3PDA,2TOF,1PA,1TA+VSD)
●13 corrective surgery
●12 large defect
●7 small defect

❖Portal (n=14)
❖Haemolytic anaemia (n=3)
❖Drugs (n=2)
❖Familial (n=2)

*RHC not performed in 26 pts with PAH-Congenital

**Figure 5** Flow chart demonstrating patient inclusion.

effusions. These features are not surprisingly associated with a poor outcome.

Ground glass attenuation is described in patients with PH.[3] Our results show that GGO is seen in all major subgroups of PAH. Centrilobular pattern of GGO correlated with poor outcome following treatment in patients with PAH in a previous study.[4] In our study, this prognostic observation was restricted to IPAH and was not seen in other major subgroups. We found a lower prevalence of GGO/septal lines in PAH-SSc than may have been expected but this reflects the rigorous way that patients with SSc with coexisting lung disease are excluded in the ASPIRE Registry, with this group having an FVC of 95 ±14% (see online supplement).

So how does an appreciation of CT characteristics in PAH help the physician? First, although there is overlap in the different forms of PAH, the presence of a ground glass pattern affecting the central part of the lung and sparring the periphery with oesophageal dilation should raise the possibility of underlying systemic sclerosis, whereas a centrilobular ground glass pattern with a very large PA and luminal calcification should suggest the possibility of an underlying congenital heart problem and prompt further investigation to confirm or refute these diagnoses. Second, the presence of adverse prognostic features on CT

such as the presence of a pleural effusion, septal lines or a dilated IVC should alert the physician that the patient falls into a poor prognostic group prompting urgent referral for specialist assessment and treatment. Given that CT results in radiation exposure and there are other validated biomarkers which are sensitive to change, its use in follow-up is not recommended. Whether a reduction in IVC area or resolution of pleural effusions/septal lines is of prognostic importance is not answered by this study. Finally, a centrilobular ground glass pattern is very common in PAH and its presence should alert the physician to the possibility of PAH if the scan was performed for unexplained breathlessness and be a prompt to look for other CT features such as PA and RV enlargement, which are seen in PH.

There are limitations to our study. We used non-gated axial images. However, the purpose of our study was to evaluate uncomplicated measurements in a non-gated CT frequently performed as a first line examination. Second, pulmonary veno-occlusive disease (PVOD) has several overlapping clinical and pathological features with IPAH, which are difficult to recognise without lung biopsy or transplantation. It is possible that patients with PAH in our cohort may have had PVOD, although the number of patients found to have histological evidence of PVOD in a previous study at postmortem was low.[5] In this
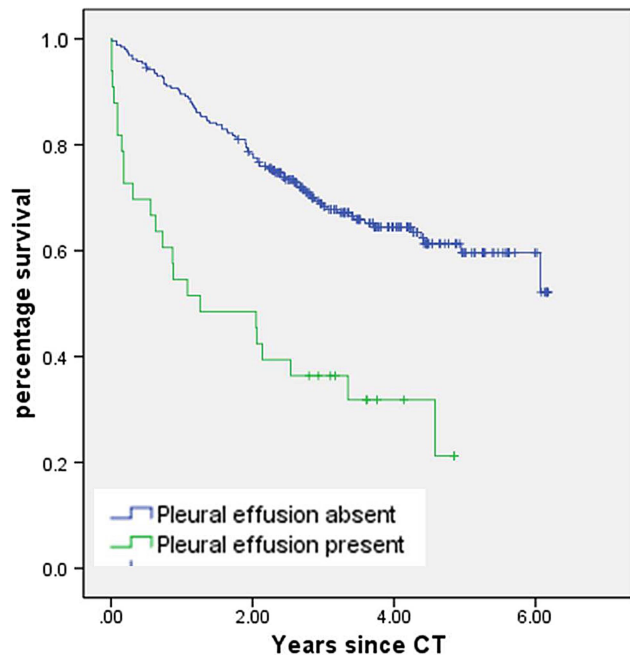
Figure 6 Kaplan–Myer curve demonstrating survival based on the presence/absence of pleural effusion.

cohort of patients, the majority of patients were in WHO functional capacity III and IV, comparable with the majority of Registry data from this era. Some more recent reports have identified a higher proportion of patients with earlier stage disease.

In conclusion, we report features of PAH and its major subgroups on a pretreatment CT and demonstrate that CT measures including the presence of pleural effusion/septal lines and inferior vena caval area predict outcome. Finally, GGO is commonly seen in PAH and its presence on a CT performed for breathlessness should raise the possibility of this diagnosis.

REFERENCES

1 Hurdman J, Condliffe R, Elliot CA, et al. Aspire Registry: assessing the spectrum of pulmonary hypertension identified at a referral centre. *Eur Respir J* 2012;39:945–55.
2 Nagueh SF, Kopelen HA, Zoghbi WA. Relation of mean right atrial pressure to echocardiographic and Doppler parameters of right atrial and right ventricular function. *Circulation* 1996;93:1160–9.
3 Sherrick AD, Swensen SJ, Hartman TE. Mosaic pattern of lung attenuation on CT scans: frequency among patients with pulmonary artery hypertension of different causes. *AJR Am J Roentgenol* 1997;169:79–82.
4 Resten A, Maitre S, Humbert M, et al. Pulmonary arterial hypertension: thin-section CT predictors of epoprostenol therapy failure. *Radiology* 2002;222:782–8.
5 Resten A, Maitre S, Humbert M, et al. Pulmonary hypertension: CT of the chest in pulmonary venoocclusive disease. *AJR Am J Roentgenol* 2004;183:65–70.

CT features of pulmonary arterial hypertension and its major subtypes: a systematic CT evaluation of 292 patients from the ASPIRE Registry

S Rajaram, AJ Swift, R Condliffe, C Johns, CA Elliot, C Hill, C Davies, J Hurdman, I Sabroe, JM Wild, DG Kiely

METHODS

ASPIRE Registry [1] is a large single centre registry of patients referred to a high volume pulmonary hypertension referral centre. All patients in this registry underwent systematic evaluation including echocardiography, detailed blood tests, exercise tolerance test, lung function test, and depending on clinical features oximetry, isotope perfusion scintigraphy, high resolution CT, CT pulmonary angiography(CTPA) and right heart catheterization(RHC). Institutional review board approval from the North Sheffield Ethics Committee was obtained for retrospective review of routinely collected patient data and written patient consent was not required.

Right Heart Catheterization: RHC was performed using a 7 French Swan-Ganz catheter. The form of PAH was classified according to standard criteria (3) and required at right heart catheter a mPAP≥25 mmHg and a PCWP≤15 mmHg.

CT Pulmonary Angiography: CTPA was performed on a 64 slice MDCT scanner (Light-Speed General Electric Medical Systems, Milwaukee, WI). Standard acquisition parameters were used: 100mA with automated dose reduction, 120kV, pitch 1, rotation time 0.5s and 0.625mm collimation. The field of view was 400x400mm with an acquisition matrix of 512x512. 100ml of intravenous contrast

agent (Ultravist 300; Bayer Schering, Berlin, Germany) was administered at a rate of 5ml/sec. HRCT were reconstructed using the contrast enhanced acquisitions with 1.25 mm collimation from the apex of the lung to the diaphragm.

Image analysis and interpretation: Scans were analyzed by a chest radiologist blinded to haemodynamic parameters, clinical findings and outcome. The mutlislice CTPA images were reviewed on dedicated PACS workstations. A second radiologist independently analysed 50 random images.

Vascular changes: Pulmonary artery: aorta ratio (PA/Ao ratio) and the maximum depth of pericardial effusion were measured as previously described (9, 10) (Figure 1). Reflux of contrast into the hepatic veins was assessed using five grades of regurgitation[2] (Figure 2). Inferior vena cava (IVC) size was measured by calculating the cross sectional area of the IVC above the level of the diaphragm, below the right atrium.

Cardiac changes: The maximum mid-transverse diameters of the right and left ventricular cavities were measured in the axial plane at their widest points between the inner surfaces of the free wall and the interventricular septum (IV septum) (Figure 3A). This may lie at different levels. Using these measurements ratio of right to left ventricle (RV/LV ratio) was obtained [3]. From the axial mid-chamber view, right atrial length was measured from the centre of tricuspid annulus to the superior right atrial wall (figure 3B). The size of the right atrium was also qualitatively evaluated using a simple 3 point visual scale: mild, moderate and severe. Displacement of the IV septum was evaluated on a three-point scale as normal septum(i.e. convex toward the right ventricle), flattened septum(straight) and deviated septum(i.e. convex toward the left ventricle) [4]. Thickness of the right ventricular free wall was recorded from the axial images[5].

Parenchymal and mediastinal changes: Ground glass opacification (GGO) was defined as increased opacity of the lung parenchyma without obscuring the pulmonary vessels or bronchi. When GGO was present the pattern was noted as centrilobular, panlobular homogenous, panlobular heterogenous according to Engeler et al[6] (Figure 4). The distribution and extent of GGO was recorded using a system described by Resten et al[7] as upper, lower or random and whether the distribution was random, subpleural or central.

CT scans were also assessed for the presence of fibrosis[8], pleural effusions, mediastinal lymphadenopathy(defined as the transverse lymnphode diameter was greater than 10 mm), dilated bronchial collaterals (defined as transverse vessel diameter greater than 2 mm)[9], septal lines[7] and oesophageal dilatation.

Statistics:

Statistical analysis was performed using PASW Statistics v16(SPSS, Chicago, IL). Continuous variables were presented as mean and standard deviation. Comparisons of continuous variables were performed with analysis of variance (ANOVA) with Bonferroni correction. Categorical variables are presented as number and percentage and compared using Chi-square test. Pearson coefficients were used to examine the correlation of continuous quantitative findings. Prognostic value of CT signs and of baseline characteristics was assessed by means of both univariate and multivariate Cox proportional hazards using forward stepwise model. Collinearity was assessed using linear regression model. Multivariable analysis was performed using all variables with a P<0.2 in the univariate model. The agreement between the two readers for the presence or absence of categorical CT findings was evaluated using the κ statistic, as described by Landis and Koch [10]. A κ value of 0−0.20 indicates slight agreement; 0.21−0.40, fair agreement; 0.41−0.60, moderate

agreement; 0.61–0.80, substantial agreement; and 0.81–1.00, almost perfect agreement.

RESULTS

Table 2 summarizes baseline hemodynamic and demographic characteristics for the 5 main subgroups of PAH. The data for the patients who had CT scanning available for review or performed within 3 months of right heart catheterisation (292) was compared to the 442 patients for demographic, functional and hemodynamic characteristics and there was no significant difference between the two data sets.

Survival results:

The maximal duration of follow up was 6 years with a mean follow-up of 3 years. During this period there were 112 deaths.

For PAH as a group, univariate Cox regression analysis demonstrated that cardiac parameters of RV/LV ratio, right atrial size, deviation of interventricular septum and presence and depth of pericardial effusion to predict outcome. Reflux of contrast into the distal hepatic veins and size of IVC and lung changes of septal lines, presence of pleural effusion and mediastinal lymphadenopathy also predicted poor outcome in patients with PAH. Multivariable Cox proportional hazard analysis incorporating clinical, hemodynamic and CT parameters showed that of CT parameters that inferior vena area and the presence of pleural effusion/septal lines were all significant (p<0.05) predictors of death and there was a trend for RV:LV ratio (p=0.06).

TABLES:

Table 2: Characteristics of Study population

Characteristics	PAH	IPAH	PAH-SSc	PAH-CHD	PAH-CTD nonSSc	PAH-Portal
No. of patients	292	74	95	63	39	14
Age (yrs)	62 (16)	62 (16) †‡	69 (9) *†#	51 (18) *#‡	60 (16) †‡	59 (12)
Female (%)	73	59‡#	85*	71	84*	64
WHO III/IV (%)	62:11	69: 12	69: 13	59: 10	74: 10	64:-
FVC (%)	89 (19)	95 (11) †	95 (14) †	72 (23) *‡§#	85 (18) †	94 (20) †
FEV1 (%)	74 (20)	83 (15) #†	80 (17) †	64 (20) *‡§	73 (17) *	77 (18) †
TLCO (%)	55 (23)	50 (19)†‡	37 (16) †§*	71 (23) *‡#	48 (8) †§	66 (7) #‡
mRAP (mmHg)	9 (5)	10 (6) #‡	6 (5) *	-	7 (4) *	9 (7)
mPAP (mmHg)	46 (14)	51 (11) #‡	42 (14) *	-	43 (11) *	47(10)
PCWP (mmHg)	10 (4)	10 (3)	10 (4)	-	9 (4)	11 (2)
CI (L.min.m2)	2.8 (0.9)	2.4 (0.7) #‡§	3 (0.83)*	-	3.2 (1.03)*	3.4 (0.8)*
PVR (woods unit)	8.7 (5.3)	11.1 (5.2)	7.1 (4.7)	-	7.3(5.0)	6.0 (2.5)
mVO2 (%)	65 (9)	62 (7)	66 (9)	-	65 (8)	70 (8)
ISWD (m)	185 (160)	176 (179) †‡	166 (137) *†#	213 (123) *‡	130 (95) ‡	236 (126)

Data shown is expressed as mean (standard deviation) * p<0.05 in comparison to IPAH, † p<0.05 in comparison to PAH-CHD, # p<0.05 in comparison to PAH-CTD-non-SSc, ‡ p<0.05 in comparison to PAH-SSc, § p<0.05 in comparison to PAH-Portal. PAH: pulmonary arterial hypertension, IPAH: idiopathic pulmonary arterial hypertension, PAH-SSc PAH in association with systemic sclerosis, PAH-CHD: PAH in association with congenital heart disease, PAH-CTD-nonSSC: PAH associated with connective tissue diseae excluding SSc, PAH-portal: PAH in association with portal hypertension, WHO: World Health Organisation Functional Class, FVC: forced vital capacity, FEV1: Forced expired volume in one second, TLco: gas transfer for carbon monoxide, mRAP: mean right atrial pressure, mPAP mean pulmonary arterial pressure, PCWP: pulmonary capillary wedge pressure, CI: cardiac index, PVR: pulmonary vascular resistance, mVO2: oxygen saturation in the pulmonary artery, ISWD: incremental shuttle walking test distance.

Table 3: Demographic, Haemodynamic and CT predictors of outcome in PAH

Parameters	Univariate HR(CI)	P-value	Multivariate HR(CI)	P-value
Age (years)	1.04(1.02-1.05)	<0.001	1.06(1.02-1.07)	0.001
Gender	0.9(0.60-1.37)	0.65		
WHO classification	1.68(1.35-2.08)	<0.001	1.11(1.70-1.08)	0.01
mRAP (mmHg)	1.01(0.98-1.05)	0.39		
mPAP (mmHg)	0.99(0.98-1.01)	0.91		
CI (L.min.m2)	0.72(0.73-0.94)	<0.019	2.1(1.45-3.03)	<0.001
PVR (dyn.s.cm-5)	1.10(1.00-1.21)	<0.002	1.0(1.00-1.02)	0.17
mVO2 (%)	0.95(0.95-0.98)	<0.001	0.90(0.94-1.01)	0.31
TLCO	0.70(0.60-0.82)	<0.001	0.31(0.12-0.66)	0.003
Cardiac signs				
PA/Ao ratio	0.49(0.24-1.10)	0.09	0.41(0.70-2.3)	0.32
RV/LV ratio	2.59(1.89-3.57)	0.05	1.87(0.95-3.70)	0.06
RA size	1.35(1.17-1.56)	0.011	1.03(0.89-1.37)	0.36
RV hypertrophy	1.00(0.94-1.06)	0.96		
IV septal position				
Normal	Reference		Reference	
straightening	1.49(0.91-2.42)	0.020	1.28(0.89-2.41)	0.13
Deviated	3.10(1.98-4.86)	0.016	2.12(1.91-3.86)	0.11
Pericardial effusion				
presence	1.65(1.17-2.47)	0.010	0.78(0.30-2.03)	0.61
Depth	1.71(1.28-2.11)	<0.05	1.37(0.91-2.69)	0.09
Vascular signs				
IVC size	1.0(1.00-1.002)	0.003	1.10(1.00-1.20)	0.033
Hepatic vein reflux				
None	Reference			
trace into IVC	1.40(0.73-2.50)	0.25		
proximal hepatic vein	1.45(0.83-2.52)	0.19		
mid hepatic vein	1.27(0.63-2.53)	0.49		
distal hepatic vein	1.79(1.05-3.06)	0.03	1.54(0.83-3.70)	0.45
Collaterals	0.55(0.28-1.10)	0.09	0.47(0.10-2.30)	0.35
Lung signs				
GG nodules				
Present	1.00(0.69-1.47)	0.96		
extent <1/3rd	Reference			
1/3rd-2/3rd	0.88(0.39-1.98)	0.75		
>2/3rd	0.95(0.45-2.01)	0.89		
centrilobular	1.04(0.57-1.86)	0.91		
central	1.71(0.72-4.04)	0.22		
Pleural effusion	3.21(2.05-5.08)	<0.001	2.09(1.02-4.31)	0.04
Septal lines	2.64(1.78-3.95)	0.001	1.34(1.10-2.15)	0.02
Lymphadenopathy	1.71(1.13-2.60)	0.016	0.71(0.38-1.32)	0.28

Table 4: CT predictors of outcome by PAH subgroup (on-line supplement)

Parameters	IPAH		PAH-SSc		PAH-CTD-nonSSc		PAH-CHD	
	P value	HR(CI)	P value	HR(CI)	P value	HR(CI)	P value	HR(CI)
Cardiac signs								
PA/Ao ratio	0.23	0.29 (0.41-2.13)	0.68	1.45(0.23-9.13)	0.62	0.48(0.03-7.72)	0.63	1.31(0.43-3.97)
RV/LV ratio	<0.05	2.31(1.33-4.01)	<0.05	2.57(1.59-4.17)	<0.05	4.79(1.30-17.60)	0.08	3.04(0.85-10.88)
RA size	<0.05	2.07(1.47-2.93)	<0.05	1.38(1.08-1.77)	<0.05	1.51(1.03-2.23)	<0.05	1.46 (0.98-2.17)
RV hypertrophy	0.23	1.09(0.94-1.27)	<0.05	1.22(1.04-1.43)	0.23	1.08(0.95-1.24)	0.82	1.01(0.89-1.16)
IV septal position								
normal		Reference		Reference		Reference		Reference
straightening	0.29	1.75(0.61-4.99)	<0.05	2.58(1.23-5.41)	0.09	1.07(0.31-3.65)		1.13(0.41-3.75)
deviated	<0.05	4.11(1.49-11.29)	<0.05	3.63(1.66-7.93)	<0.05	3.69(1.26-10.71)		4.04(1.09 -14.97)
Pericardial effusion								
presence	0.11	1.76(0.88-3.51)	<0.05	2.75(1.44-5.26)	0.09	1.50(0.59-3.83)	0.29	0.49(0.14-1.81)
depth	<0.05	1.67(1.02-1.71)	<0.05	1.08(1.04-1.13)	0.14	1.12(0.96-1.09)	0.71	0.98(0.90-1.07)
Vascular signs								
IVC size	<0.05	1.26(1.09-1.45)	<0.05	1.14(1.01-1.92)	<0.05	1.23(1.02-1.49)	0.80	1.00(0.99- 1.00)
Hepatic vein reflux								
None		Reference		Reference		Reference		Reference
trace into IVC	0.39	1.71(0.49-5.94)	0.67	1.17(0.27-2.33)	0.65	1.28(0.42-3.94)	0.92	1.23(0.51-3.91)
proximal hepatic vein	0.39	1.79(0.59-5.36)	<0.05	1.31(0.41-4.25)	0.67	0.71(0.15-3.37)	0.93	0.63(0.17-2.27)
mid hepatic vein	0.17	2.28(0.69-7.53)	0.64	2.29(0.98-5.35)	0.31	0.34(0.04-2.75)	0.93	0.45(0.14-1.85)
distal hepatic vein	0.38	1.69(0.55-5.17)	<0.05	6.13(2.59-15.07)	0.80	1.21(0.25-5.78)	0.92	1.54(0.53-4.68)
Collaterals	0.95	1.03(0.32-3.40)	0.56	1.21(1.01-5.61)	0.45	0.56(0.13-2.47)	0.62	0.74(0.22-2.43)
Lung signs								
GG nodules								
presence	0.86	0.94(0.47-1.89)	0.31	1.37(0.74-2.57)	0.33	1.63(0.61-4.36)	0.94	1.04(0.34-3.18)
Centrilobular	0.03	3.45(1.19-10.67)	0.41	1.55(0.55-4.43)	0.08	6.9(0.78-62.38)	0.06	4.13(0.94-19.15)
Central	0.42	0.04(0.01-73.35)	0.08	0.33(0.11-0.94)	0.94	0.92(0.10-8.36)	0.65	0.05(0.00-33.06)
Pleural effusion	<0.05	3.68(1.73-8.62)	<0.05	3.06(1.49-6.31)	<0.05	2.87(0.55-3.94)	<0.05	4.55(1.0-20.16)
septal lines	<0.05	2.57(1.29-5.15)	0.18	1.55(0.81-2.97)	0.91	1.12(0.15-8.47)	0.14	2.44(0.74-8.01)
Lymphadenopathy	<0.05	3.42(1.66-7.07)	0.36	1.41(0.67-2.99)	0.60	1.29(0.49-3.46)	0.24	4.69(1.22- 17.97)

REFERENCE:

1. Hurdman J, Condliffe R, Elliot CA, et al. Aspire Registry: assessing the spectrum of pulmonary hypertension identified at a referral centre. Eur Respir J 2011 doi: 09031936.00078411 [pii]
10.1183/09031936.00078411[published Online First: Epub Date]|.
2. Groves AM, Win T, Charman SC, Wisbey C, Pepke-Zaba J, Coulden RA. Semi-quantitative assessment of tricuspid regurgitation on contrast-enhanced multidetector CT. Clin Radiol 2004;**59**(8):715-9 doi: 10.1016/j.crad.2004.02.007
S0009926004000753 [pii][published Online First: Epub Date]|.
3. van der Meer RW, Pattynama PM, van Strijen MJ, et al. Right ventricular dysfunction and pulmonary obstruction index at helical CT: prediction of clinical outcome during 3-month follow-up in patients with acute pulmonary embolism. Radiology 2005;**235**(3):798-803 doi: 2353040593 [pii]
10.1148/radiol.2353040593[published Online First: Epub Date]|.
4. Reid JH, Murchison JT. Acute right ventricular dilatation: a new helical CT sign of massive pulmonary embolism. Clin Radiol 1998;**53**(9):694-8
5. Remy-Jardin M, Remy J, Wattinne L, Giraud F. Central pulmonary thromboembolism: diagnosis with spiral volumetric CT with the single-breath-hold technique--comparison with pulmonary angiography. Radiology 1992;**185**(2):381-7
6. Engeler CE, Tashjian JH, Trenkner SW, Walsh JW. Ground-glass opacity of the lung parenchyma: a guide to analysis with high-resolution CT. AJR Am J Roentgenol 1993;**160**(2):249-51
7. Resten A, Maitre S, Humbert M, et al. Pulmonary arterial hypertension: thin-section CT predictors of epoprostenol therapy failure. Radiology 2002;**222**(3):782-8
8. Devaraj A, Wells AU, Meister MG, Corte TJ, Hansell DM. The effect of diffuse pulmonary fibrosis on the reliability of CT signs of pulmonary hypertension. Radiology 2008;**249**(3):1042-9 doi: 249/3/1042 [pii]
10.1148/radiol.2492080269[published Online First: Epub Date]|.
9. Remy-Jardin M, Duhamel A, Deken V, Bouaziz N, Dumont P, Remy J. Systemic collateral supply in patients with chronic thromboembolic and primary pulmonary hypertension: assessment with multi-detector row helical CT angiography. Radiology 2005;**235**(1):274-81 doi: 2351040335 [pii]
10.1148/radiol.2351040335[published Online First: Epub Date]|.
10. Landis JR, Koch GG. The measurement of observer agreement for categorical data. Biometrics 1977;**33**(1):159-74

FIGURE LEGENDS:

Figure 1: The pulmonary artery (PA) aorta ratio was obtained by measuring the widest transverse diameter of the PA (blue) and the corresponding transverse diameter of aorta (red).

Figure 2: Grading of tricuspid regurgitation (A) 0 = there is no reflux into IVC, (B) 2 = reflux into IVC but not hepatic veins, (C) 3 = reflux into IVC and proximal hepatic veins (D) 4 = reflux into IVC and distal hepatic veins

Figure 3: (A) The maximum mid-transverse diameters of the RV (blue arrow) and LV (left arrow) cavities were measured in the axial plane at their widest points between the inner surfaces of the free wall and the interventricular septum. (B) For assessing the right atrial size on CT, right atrial length was measured from the centre of tricuspid annulus to the superior right atrial margin

Figure 4: Centrilobular ground glass pattern (A) and central ground glass pattern (B)

Figure 5: Flow chart demonstrating patient inclusion

Figure 6: Kaplan-Myer curve demonstrating survival based on the presence/absence of pleural effusion